Numerical simulation of quasi-geostrophic turbulence

By H. LEONARD STEINBERG,[1] *Department of Environmental Sciences, Tel-Aviv University, Ramat Aviv, Israel*

(Manuscript received September 12; revised version December 27, 1972)

ABSTRACT

The development of turbulence is studied numerically through the use of a simplified two-level quasi-geostrophic model. The domain occupied by the fluid has 64×64 grid points in the horizontal and obeys cyclic boundary conditions in the x- and y-directions. The turbulence is generated by a heating function composed of the 2-dimensional fourier components having the larger wave number, $m = 8$. Three cases are investigated for two values of H, the amplitude of the heating function and two values of ν, the coefficient of eddy viscosity. Quasistationary spectra are obtained in each case. The slopes of the spectra for $8 \leqslant m \leqslant 16$ on a log–log graph vary from -1.7 to -3.4 depending on ν and H. The nonlinear cascade of available potential energy is found to be toward larger wavenumbers. The nonlinear cascade of kinetic energy is from components for which $8 \leqslant m \leqslant 14$, mainly toward $1 \leqslant m \leqslant 7$, the larger scales. The gains for $m > 14$ resulting from the cascade is relatively small. These transfers are in qualitative agreement with atmospheric observations. Gains of enstrophy are observed to be fairly constant for $14 \leqslant m \leqslant 28$. In an inertial subrange they should be zero. Relatively small gains are recorded for $m < 7$ while the spectral region $8 \leqslant m \leqslant 14$ acts as source. Except for the wavenumber of transition from negative to positive values the distribution of losses and gains of enstrophy due to the inertial cascade is similar to that resulting from calculations based on atmospheric observations. It is concluded that the two dimensional turbulence theories enunciated by Fjørtoft, Kraichnan and Leith pertain to the model in this study and the atmosphere (so far as our model resembles the atmosphere) in the prediction of the dominant direction of the nonlinear cascades of kinetic energy and enstrophy in wavenumber space. Inertial subranges in which the cascades result in zero changes are neither observed in the numerical experiments of this study nor in calculations based on atmospheric observations in the spectral region $8 \leqslant m \leqslant 16$. The experiments described in this paper were performed prior to the theory proposed by Charney and so were not designed to be a test of it. However, some assumptions and conclusions are discussed in the light of that theory.

1. Introduction

In recent years atmospheric observations have yielded kinetic energy spectra (Ogura, 1958; Horn & Bryson, 1963; Wiin-Nielsen, 1967; Julian et al., 1970), which seem to obey a power law of about -3 for $8 \leqslant m \lesssim 16$ (m is the non-dimensional planetary wave number). Similar results are obtained from General Circulation Studies (Manabe et al., 1970; Wellck et al., 1971). At about the same time, theoretical studies (Kraichnan, 1967; Leith, 1969; Batchelor, 1969) show that a -3 power law for kinetic energy and a -1 power law for enstrophy is consistent with the assumption of an enstrophy cascading intertial subrange in a two-dimensional isotropic, homogeneous, incompressible turbulent fluid flow.

It is very tempting to use the quasi-two-dimensionality of the large scale atmospheric circulation to link the theories with the atmospheric observations. However, the calculations available (Yang, 1967; Saltzman & Teweles, 1964; Wiin-Nielsen, 1959) indicate that although the large scale flow may be two-dimensional with respect to accelerations and velocities, it is not so with respect to the energetics. The baroclinic process, $C(A_e, K_e)$, of conversion of eddy available potential energy, A_e, to eddy kinetic energy, K_e, by overturning in the zonal plane dominates the nonlinear cascade of

[1] This work was done while at the Department of Meteorology and Oceanography, Ann Arbor, Michigan.

energy, $C_K(m/n, l)$ in the spectral subrange which seems to be governed by the -3 power law. (n and l are the set of permitted wavenumbers.) Further inconsistencies in the application of the two-dimensional turbulence theories to the atmosphere are discussed by Charney (1971) (hereafter referred to as C). In C an argument is put forth based on the quasi-geostrophic nature of the large-scale atmospheric flow ($8 \leq m \leq 16$) which again results in the prediction of a -3 power law. The work presented in this paper was performed prior to the enunciation of the Geostrophic Turbulence Theory by Charney and is not a test of that theory. It is of interest, however, to discuss the model used here and the results obtained in the light of that theory.

2. The –3 power play

Two questions to which the present paper addresses itself are:

1) *Is the -3 power for the kinetic energy in the spectral region under concern unique?* and

2) *If it is not unique on what may it depend?*

In connection with the first question it is interesting to note that the first numerical simulations of two dimensional turbulence (Lilly, 1969) did yield a -3 power law for the kinetic energy and a corresponding -1 power law for enstrophy (Batchelor, 1969) for $m > m_i$ (m_i is the wavenumber of energy input). Subsequent simulations (Deem & Zabusky, 1971), however, show that various regimes may be identified in ν (coefficient of viscosity) and λ (microscale wavelength) space. In the atmosphere (Ogura, 1958; Horn & Bryson, 1963; Julian et al., 1970; Wiin-Nielsen, 1967; Kao, 1970) the power is seen to vary from about -2 to -4 depending on pressure, latitude, and time. In a general circulation model (Manabe et al., 1970), which obviously does not have an inertial subrange in the spectral region $8 \leq m \leq 16$, a -3 power law is obtained.

We have, therefore, (a) numerical simulations in which an inertial subrange may exist but a power law differing from -3 is found, (b) a numerical simulation without an inertial range (both viscosity and the baroclinic energy conversion dominate the nonlinear transfer) in which a -3 power is found, and (c) the atmosphere which, at least for $8 \leq m \leq 10$ (Baer, 1972) and probably up to $m = 15$ (Yang, 1967), cannot be considered to be an inertial subrange, with exponents in the neighbourhood of -3 but ranging between about -2 and -4.

0	P = o cb	$\omega_o = 0$
1	25	$\frac{\partial}{\partial t} q_1 = -\vec{V}_1 \cdot \nabla q_1 + \nu \nabla^2 q_1 + H$
2	50	$\frac{f_o \omega_2}{P_2} = \lambda^2 [(\frac{\partial}{\partial t} + \vec{V}_2 \cdot \nabla) T + \frac{H}{\lambda^2} - \nu \nabla^2 T]$
3	75	$\frac{\partial}{\partial t} q_3 = -\vec{V}_3 \cdot \nabla q_3 + \nu \nabla^2 q_3 - H$
4	100	$\omega_4 = 0$

Fig. 1. Schematic of model's vertical resolution, equations and vertical boundary conditions.

The question of the dependency of the spectral slope on the amplitude of energy input, H, and eddy viscosity coefficient, ν, is only briefly investigated here by three simulation experiments using two values of H and two of ν. The number of experiments was limited, in part, by the computer time required. A run of 1 500 time steps uses about 80 min on a CDC 6600.

3. The model

The tool used in this study is a modified version of Phillips (1956) quasi-geostrophic model. The general development will be omitted and only the modifications will be discussed here. The energy input is through a heating function which is identical to the forcing function used by Lilly (1969). The lateral domain is one of an infinite number of identical contiguous squares. Each square, therefore, has cyclic lateral boundary conditions. Fig. 1 shows the vertical resolution vertical boundary conditions and the prognostic equations for the geostrophic potential vorticity.

The notation in Fig. 1 is similar to Phillips (1956) and is as follows[1]:

$$q_1 = \nabla^2 \psi_1 - \lambda^2 T$$

$$q_3 = \nabla^2 \psi_3 + \lambda^2 T$$

q is the potential vorticity
ψ is the stream function
ν is the eddy viscosity coefficient

[1] Place note change in definition of λ.

Table 1. *Scale restrictions and assumptions used in geostrophic turbulence theory, and typical values taken from Case A*

Scale restrictions	Typical values
1. $k_H u_k/f_0 < 0(1)$	0.6
2. $f_0^2 k_v/k_H^2 g < 0(1)$	0.5
3. $k_H/k_v \leqslant 0(R_0)^2$	$10^{-3} < 10^{-2}$
4. $(a\,k_H)^{-1} \leqslant 0(R_0)$	$0.075 < 0.1$
5. $k_v > 0(\ln \bar{\theta})_z$	$2 \times -10^{-3} > 10^{-4}$
Additional Assumptions	
1. $\lambda_H, \frac{N}{f_0}\lambda_v < 2\lambda \left(= \frac{2HN}{f_0}\right)$	3×10^6m, 0.5×10^6m $\leqslant 3.4 \cdot 10^6$m
2. $k_H^2 u_k \gg \beta$	$1.3 \times 10^{-10} > 1.6 \times 10^{-11}$

T is a measure of the thermal field $(= \psi_1 - \psi_3)$

$$\lambda^2 = f_0^2 \theta_2 \,|\, (\psi_3 - \psi_1)\,(\theta_3 - \theta_1)\,|^{-1} = 1.6 \times 10^{-12}\ m^{-2}$$

θ is the potential temperature (°K)

$\mathbf{v}_1$, $\mathbf{v}_2$, $\mathbf{v}_3$ are the horizontal velocity vectors for surface 1, 2 and 3, resp.

$\omega\{ = dp/dt\}$ is the vertical motion in pressure coordinates

f_0 is the Coriolis parameter taken at 45° N

t is time

∇ is the two dimensional del operator $= \mathbf{i}\dfrac{\partial}{\partial x} + \mathbf{i}\dfrac{\partial}{\partial y}$

∇^2 is the Laplacian $= \left(\dfrac{\partial^2}{\partial x^2} + \dfrac{\partial^2}{\partial y^2}\right)$

$P_2 = 50$ cb

H is the amplitude of the diabatic heating other than thermal diffusion

The subscripts refer to pressure surface.

The dimensional restrictions on quasi-geostrophic turbulent flow (Charney & Stern, 1962; Charney, 1971) are tabulated in Table 1 along with typical values taken from Case A. Quantities used in these calculations are $\lambda_H \sim 3 \times 10^6$ m, $\lambda_v \sim 3 \times 10^3$ m, $f_0 \sim 10^{-4}$ sec^{-1}, $u_k \sim 30$ m sec^{-1}, $g = 9.8$ m sec^{-2}, $N = (g\,\partial \ln \theta/\partial z)^{\frac{1}{2}} \sim 1.7 \times 10^{-2}$ sec^{-1} and $\beta \sim 1.6 \times 10^{-11}$ m^{-1} sec^{-1}. The length of a side is taken equal to 28×10^6 m which is approximately the circumference of a mid-latitude circle.

It can be seen that the scale restrictions are generally obeyed. The first of the additional assumption ... "implies that the scales are small in comparison with the baroclinic excitation scales" ... This assumption is not found to hold with respect to the horizontal scale and the associated implication is not observed in both the atmosphere and in the numerical experiments to be described below. The spectral range of $8 \leqslant m \leqslant 16$ cannot be said to be far removed from the scales of baroclinic excitation in the atmosphere, the general circulation simulation (Manabe et al., 1970), or in the simulations of quasi-geostrophic turbulence contained herein.

In the light of the cyclic boundary conditions the integral effect of the β-term in the potential vorticity equation is zero. Charney's assumption that the β-term may be ignored for $k_H^2\, u_k \gg \beta$ is observed in our model and justifies omission of this term in the detailed sense as well.

The major concern of this study is the non-linear interactions between the waves. It was decided, therefore, to omit the zonal mode of motion. Although this omission distorts the resultant energetics for the very long waves $(1 \leqslant m \leqslant 7)$, the interaction between the zonal flow and the waves of larger wavenumber $(8 \leqslant m \leqslant 16)$ is observed to be small (Yang, 1967; Saltzman, 1970; Steinberg et al., 1971). This assumption is also introduced in C. The absence of the zonal mode necessitates energy introduction through the eddy modes and thus departing from the way in which energy is put into the atmosphere. Eddy available potential energy is generated, in contrast to the atmosphere in which the heating results in a generation of zonal available potential energy and $G(A_e)$, the generation of eddy available potential energy is almost everywhere negative (Lawniczak, 1969). We may expect, therefore, large differences in the energetics for $m < 8$ between the present model and the atmosphere.

The heating field is generated in the same way as the forcing function used by Lilly (1969). The fields at times t and $t + \Delta t$ are related by

$$H^{t+\Delta t} = RH^t + [1 - R^2]^{\frac{1}{2}}\, \tilde{H}^{t+\Delta t}$$

R is a correlation coefficient such that $0 \leqslant R \leqslant 1$ and Δt is the time interval used in integration of the model. This is a first order Markov process in which the statistical properties of H depends on R and Δt. $\tilde{H}$ is composed of components whose larger wavenumber is 8. The amplitudes of its spectral components are chosen randomly from a Gaussian distribution. The total amplitude of $\tilde{H}$ is kept constant by normalization and so only the phase relationships change.

Since the thermal field at any time is a function of the heating field (as well as other variables) a value of R close to zero implies little correlation between the temperature field and the newly composed heating field. Inhibition of the generation of available potential energy results. In three experiments performed in this study $R = 0.7$ was used, equally weighting H^t and $\tilde{H}^{t+\Delta t}$. Phillips (1963) gives the limitation on the heating rate consistent with the quasi-geostrophic approximation to be about 10^{-1} m^2 sec^{-3} per unit mass. The values of the heating rate associated with the values of $|H|$ used in this study are listed in Table 2 and are within the limit given by Phillips.

In the experiments conducted in this study $m_i = 8$. This corresponds closely to the spectral region of maximum baroclinic instability as given by theoretical considerations (Derome & Wiin-Nielsen, 1966). The observational studies (Saltzman & Fleisher, 1960, 1961; Wiin-Nielsen, 1959) of the conversion of eddy available potential energy to eddy kinetic energy indicate a maximum at $m \sim 6$, 7. By using $m_i = 8$ the conversion process is forced to have its maximum at $m = 8$, thereby maintaining close correspondence with the atmosphere.

The neglect of boundary friction is in accordance with the last assumption in C. We do not, however, have an inertial subrange for which "... no appreciable internal viscous dissipation occurs". The -3 power spectral range realized in the general circulation experiment (Manabe et al., 1970) also did not behave in accordance with this assumption. Although the dissipation formulation was based on an inertial range argument both the vertical and horizontal dissipation mechanisms are "significantly large at the wavenumbers of baroclinic instability". The relative importance of the horizontal and vertical dissipation changes with resolution but they have similar spectral shape. Only the horizontal dissipation was used in this study.

The first prognostic step uses a forward centered time differencing scheme while all others used the Adams-Bashfort formulation. This scheme is known to be very slightly unstable (Lilly, 1965) and was used by Lilly (1969) and Orzag (1969) with satisfactory results. The time step used for the time integration was taken to be 1 hour. The diagnostic calculations were performed every 12 time periods or 12 hours in real time. Since the diagnostic calculations are performed once for every 12 steps of the prognostic calculations we cannot expect

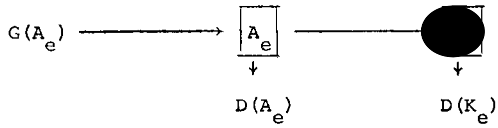

Fig. 2. Energy flow diagram for the model.

precise correspondence between the energy changes evaluated by the l.h.s. of (1) and (2), given below, and their r.h.s. An examination of the energy budgets given by these two methods over the periods of integrations yields results on the same order of those obtained by Smagorinsky (1963). (Further details are given by Steinberg (1971), hereafter denoted by A.) The advective term was approximated by Arakawa's (1966) second order formulation which conserves kinetic energy and enstrophy.

4. Energetics of the model

The formulation for the calculation of the energies and energy transformations for the model is similar to that of Phillips (1956) and is given in A. The absence of a zonal flow and area means of the stream functions, ψ_1 and ψ_3, result in the existence of only the eddy form of available potential energy and kinetic energy. The energy diagram pertinent to our model is depicted in Fig. 2.

The equations for the energy changes are:

$$\frac{\partial}{\partial t} A_e = G(A_e) + D(A_e) - C(A_e, K_e) \qquad (1)$$

$$\frac{\partial}{\partial t} K_e = C(A_e, K_e) + D(K_e) \qquad (2)$$

We are particularly interested in the nonlinear exchanges which redistribute A_e and K_e in wavenumber space. Thus, if (1) and (2) are examined as a function of wavenumber one additional term appears in each equation, i.e., the term representing the gain due to the nonlinear interactions of waves and will be denoted by $C_x(m \mid n, l)$ where x may be A_e or K_e.

We also evaluate the enstrophy and the nonlinear cascade of this quantity in wavenumber space.

The enstrophy is given by

$$\xi = \frac{1}{L^2} \int_0^L \int_0^L \frac{1}{2} \left| (\nabla^2 \psi_1)^2 + (\nabla^2 \psi_3)^2 \right| dx\, dy$$

Table 2. *Heating amplitude and coefficient of eddy viscosity*

	Case A	Case B	Case C
dQ_h/dt ($m^2\ sec^{-3}$)	0.070	0.070	0.021
$\nu(\times 10^9\ cm^2\ sec^{-1})$	0.85	1.7	0.85

The rate of enstrophy gain due to the nonlinear cascade is given by

$$\sum_{m=1}^{32} I(m\,|\,n,l) = \frac{1}{L^2}\int_0^L\int_0^L - (\xi_1 \mathbf{V}_1 \nabla\xi_1 + \xi_3 \mathbf{V}_3 \nabla\xi_3)\,dx\,dy$$

$I(m\,|\,n,l)$ is zero when integrated over the domain and only its decomposition in wavenumber space is of interest. All the terms in the energy equation are evaluated by decomposing the factors into Fourier components and calculating the products of the components. This, avoids the filtering effects of the finite difference approximations.

5. The energy cycle and nonlinear transfers

We shall use the results of Case A to illustrate the following discussion. There is an initial start up period which lasts for 200 to 300 time steps, depending upon the particular case, during which both forms of energy increase rapidly (see Fig. 3). Thereafter, the available potential energy decreases somewhat and then is quasi-stationary or very slowly decreasing with time. The eddy kinetic energy, on the other hand, continues to increase with time. The continual increase in K_e is due to growth for $m < 8$ due to the nonlinear trapping effect discussed below.

The energy input to A_e is through $G(A_e)$ at wavenumber 8. The nonlinear transfer of this quantity is predominantly toward large m. Therefore, we do not observe the loss, due to nonlinear effects, of A_e for $m < 8$ as observed in the atmosphere (Yang, 1967). The conversion from A_e to K_e, $C(A_e, K_e)$, in this spectral region should not be expected to and does not approximate atmospheric behavior.

The nonlinear gain of A_e for $m > 8$ is predominantly removed by $C(A_e, K_e)$ and to a lesser degree by $D(A_e)$ the dissipation effects. In general, for $m > 8$, $C(A_e, K_e) \sim C_A(m\,|\,n, l) +$

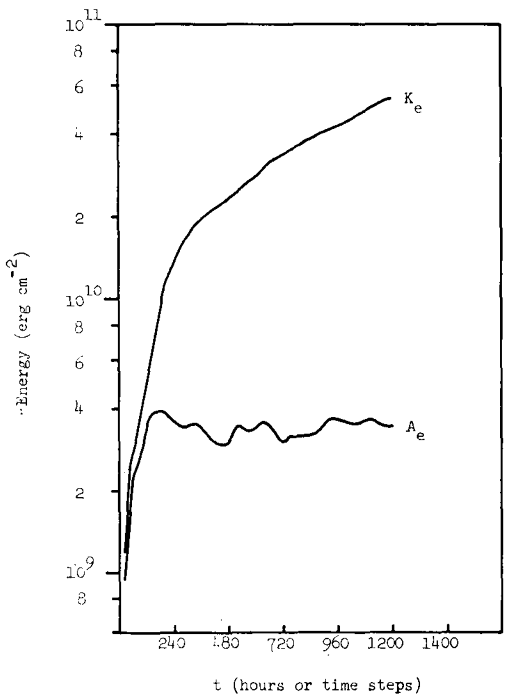

Fig. 3. K_e and A_e as a function of time for Case A.

$D(A_e)$ with $D(A_e) \sim 0.2\ C(A_e, K_e)$. The mean value of these processes for $300 \leq t \leq 1\,200$ as a function of wavenumber are exhibited in Fig. 4.

The eddy kinetic energy, K_e, in the spectral region $1 \leq m \leq 7$ receives energy by the nonlinear transfer process but our neglect of $C(K_e, K_z)$ and misrepresentation of $C(A_e, K_e)$ prevents this spectral region from resembling the atmosphere. Instead, K_e for $1 \leq m \leq 7$ in our model should more closely correspond to the two-dimensional theoretical model than the atmosphere since the nonlinear transfer dominates the energy gains. $D(K_e)$ the dissipative effect is small and $C(A_e, K_e)$ is small and has alternating sign. As the spectrum of K_e for $m \geq 8$ attains quasi-stationarity the dominant kinetic energy transfer process is that of trapping energy at $m < 8$ and chiefly at $m = 1$. The mean values of $C_K(m\,|\,n, l)$, $C(A_e, K_e)$ and $D(K_e)$ for $300 \leq t \leq 1\,200$ are shown in Fig. 5.

For $m \geq 8$, the K_e spectrum in our model should resemble the atmospheric spectrum since we account for $C(A_e, K_e)$, $C_K(m\,|\,n, l)$, and $D(K_e)$ in a reasonable fashion. $C(K_e, K_z)$, which

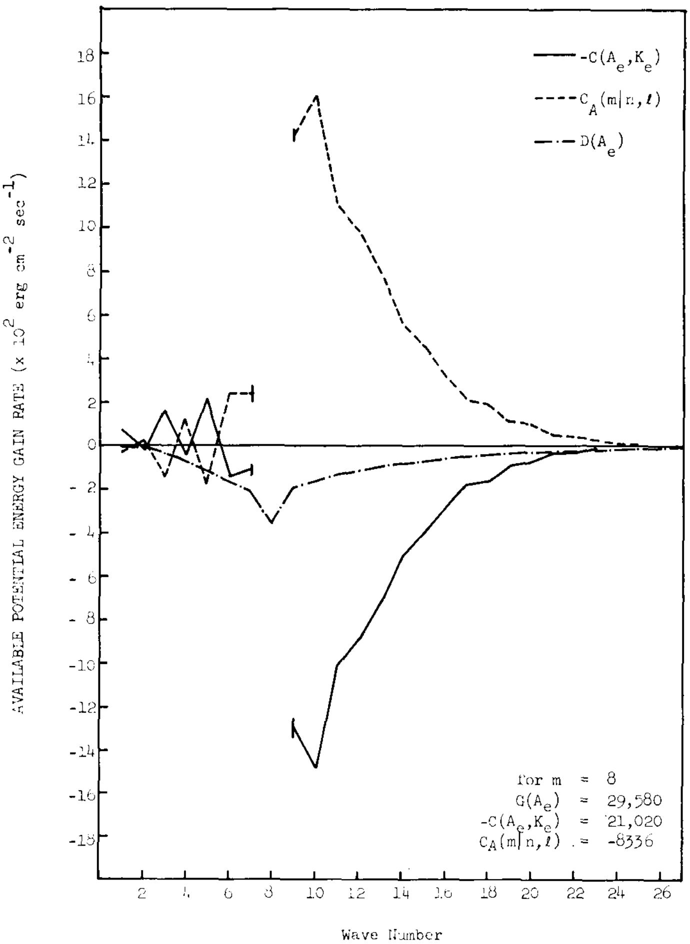

Fig. 4. Mean values of $C_A(m|n, l)$ and $D(A_e)$ for $300 \leqslant t \leqslant 1\ 200$, Case A.

is not accounted for in our model, is relatively smaller in the atmosphere for $m > 8$.

The effect of the nonlinear exchange of K_e is a loss for $8 \leqslant m \leqslant 14$ and small gains for $m > 14$. For $9 \leqslant m \leqslant 14$ a balance is achieved among $C_K(m|n, l)$, $C(A_e, K_e)$ and $D(K_e)$ with the three quantities of the same order of magnitude.

It is noted that the kinetic energy supply for $8 \leqslant m \leqslant 17$ in our model is not $C_K(m|n, l)$, but it is the balance of all the involved processes which maintain the quasi-stationary spectral slope. In the atmosphere $C(A_e, K_e)$ (Saltzman & Fleisher, 1960; Wiin-Nielsen, 1959) is larger than $C_K(m|n, l)$ (Yang, 1967) for this spectral range except perhaps the short wave end where both are small.

The nonlinear enstrophy transfer is predicted by the two-dimensional turbulence theory to be constant and toward large wave number in the postulated inertial sub-range. We find the direction of transfer to be verified in the model. The losses of enstrophy occur for $8 \leqslant m \leqslant 14$ while the gains take place mainly in the spectral region with $m > 14$. Fig. 6 depicts $I(m|n, l)$ as a function of wavenumber for Case A. The values are the means for $300 \leqslant t \leqslant 1\ 200$. There is a very close correspondence between the action of the nonlinear transfer of enstrophy in the atmosphere (Steinberg, 1971, Fig. 4) and in the model if the wavenumbers at which the sign changes are used as reference points. The exception exists for $1 \leqslant m \leqslant 7$ in the model's results.

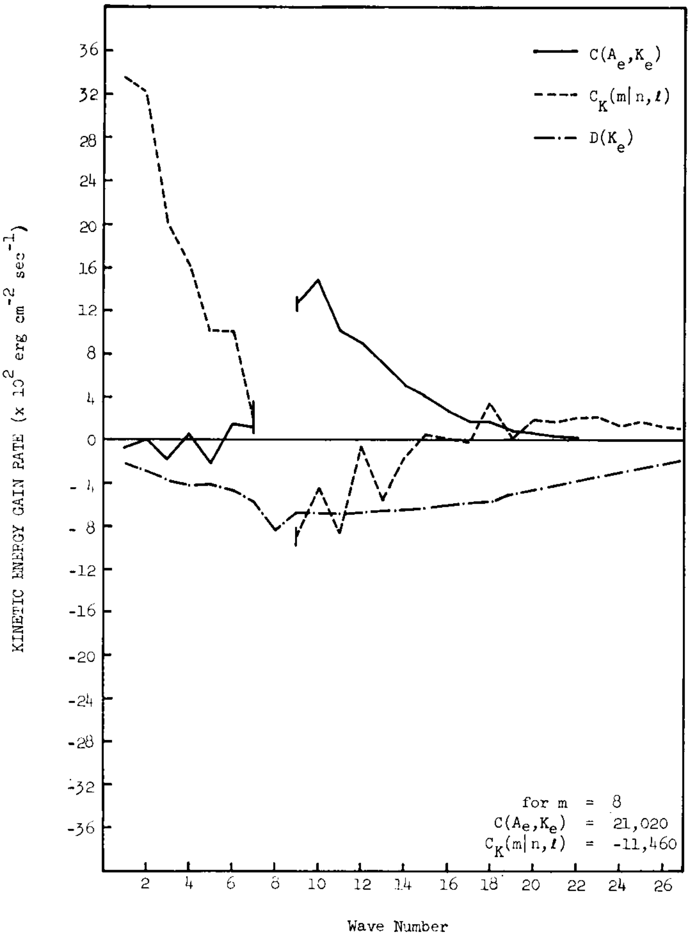

Fig. 5. Mean values for $C_K(m|n, l)$, $C(A_e, K_e)$ and $D(K_e)$ for $300 \leqslant t \leqslant 1\ 200$, Case A.

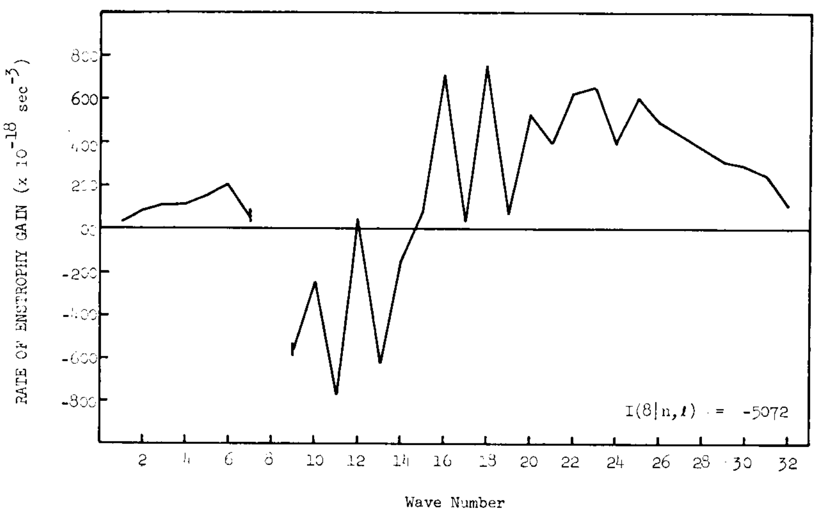

Fig. 6. Mean value of $I(m|n, l)\ 300 \leqslant t \leqslant 1\ 200$, Case A.

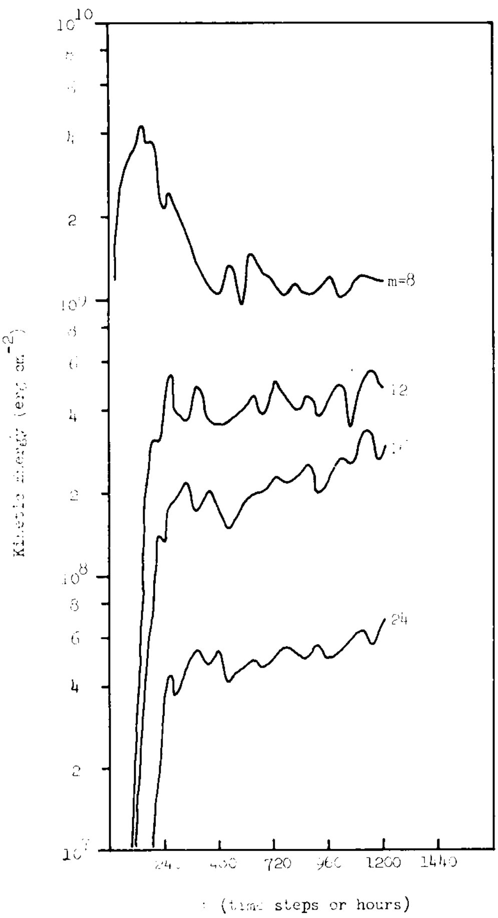

Fig. 7a. The kinetic energy of wavenumbers 8, 12, 16, and 24 as a function of time, Case A.

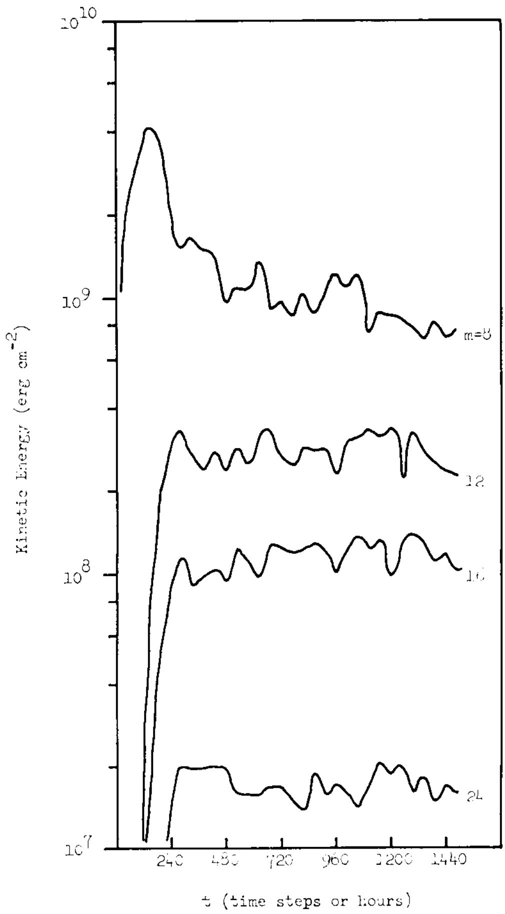

Fig. 7b. The kinetic energy of wavenumbers 8, 12, 16, and 24 as a function of time, Case B.

Since the processes in the spectral region are misrepresented (as discussed in connection with the available potential energy spectrum) this region should not and does not have correspondence with the atmospheric case.

6. "Power laws"

After the initial start up period and overshoot, the kinetic energy at each wavenumber for $m > 8$ may be described as quasi-stationary. The kinetic energy for $m = 8$, 12, 16, and 24, for Cases A, B and C are exhibited as a function of time in Figs. 7*a*, *b*, *c*, respectively. A small positive trend with time is observed for the kinetic energy at $m = 16$ and 24 for Ca e A beginning at $t = 1\ 000$. This is not observed in Cases B and C in which the quasi-stationary characteristic is more closely adhered to.

The kinetic energy spectra at $t = 600$ and 1 200 (Case A) are depicted in Fig. 8*a*. It is noted that changes for $m \geq 8$ are small whereas the major changes occur for $m < 5$ and particulary at $m = 1$, 2, due to the nonlinear trapping effect mentioned in the previous section. This holds true, if anything, to a greater degree in Cases B and C which are depicted in Figs. 8*b* and *c*. Table 3 lists the spectral slopes, calculated by least squares, of the kinetic energy for $8 \leq m \leq 16$ as a function of time for the various cases.

We have obtained three quasi-stationary kinetic energy distributions in wavenumber space (Fig. 9) by altering the relative intensity of the generation of energy and its dissipation.

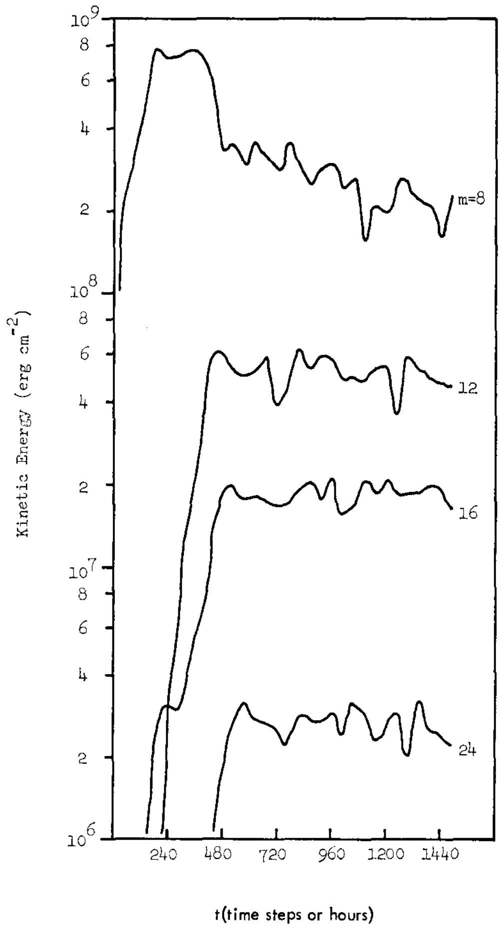

Fig. 7c. The kinetic energy of wavenumbers 8, 12, 16, and 24 as a function of time, Case C.

The nonlinear effects are generally smaller than either of the dissipation or the conversion from available potential energy. It would seem, therefore, that arguments based on the assumption of an inertial subrange are inapplicable to deducing the kinetic energy spectral slope for $8 \leqslant m \leqslant 16$ in our model and perhaps in the atmosphere as well. It is seen that both a relative increase in the viscosity coefficient and a decrease in the intensity of energy production result in relatively smaller decascades of A_e and subsequent decrease in $C(A_e, K_e)$.

The available potential energy for Cases A, B and C at $t = 1\ 200$ hours are depicted in Fig. 10. For large wavenumbers a slope of about -5 is observed. Merilees & Warn (1972) have explained this on the basis of the limited vertical resolution of the two-level model. The two level model, therefore, cannot verify the property of equipartition, between the components of the kinetic energy and the available potential energy, required by the geostrophic turbulence theory.

Table 3. *Kinetic energy spectra slopes, $8 < m < 16$ as a function of time.*

Case	Time 300	600	900	1 200	1 500
A	−3.1	−2.2	−1.8	−1.7	
B	−3.6	−3.1	−3.2	−2.8	−2.8
C	−6.6	−3.6	−3.6	−3.3	−3.4

7. Summary and conclusions

A modified quasi-geostrophic two-layer model was integrated for 1 200 to 1 500 hours depending on the case.

The energy cycle is similar to that observed in the atmosphere except in the spectral region with $m < 8$. A_e, generated at $m = 8$, is both converted to K_e and transferred, for the most part, toward components with $m > 8$. This is in agreement with the cascade direction observed in the atmosphere. The available potential energy seems to attain a quasi-stationary state by $t \sim 300$ hours and does not change much thereafter. The power-law governing the spectral distribution of A_e would require an exponent of about -5.

Available potential energy is converted into kinetic energy for all components with $m \geqslant 8$. The nonlinear transfer of K_e is from waves with $8 \leqslant m \leqslant 14$ predominantly toward the large scale portion of the spectrum. There is a relatively small transfer toward $m > 14$. After an initial period of about 300–400 time steps K_e, for $m \geqslant 8$, becomes quasi-stationary while for $m < 8$, in particular, $m = 1$, 2 growth continues by virtue of the nonlinear transfer. This portion of the spectrum seems to be approaching a $-5/3$ slope. In the atmosphere this growth is countered by the transfer of kinetic energy from the large scale eddies to the zonal mode.

In Case A, $C_K(m|n, l)$, $C(A_e, K_e)$ and $D(K_e)$

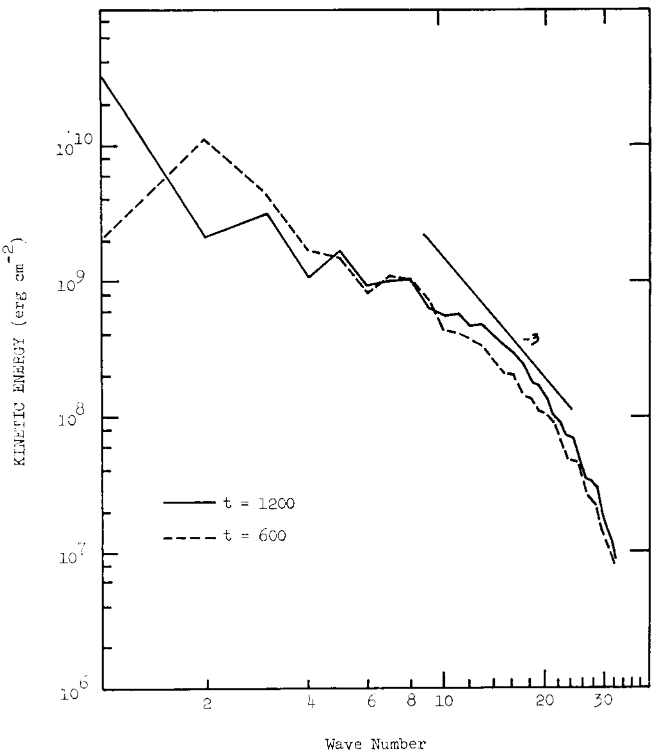

Fig. 8a. The kinetic energy spectrum number at $t = 600$ and 1 200, Case A.

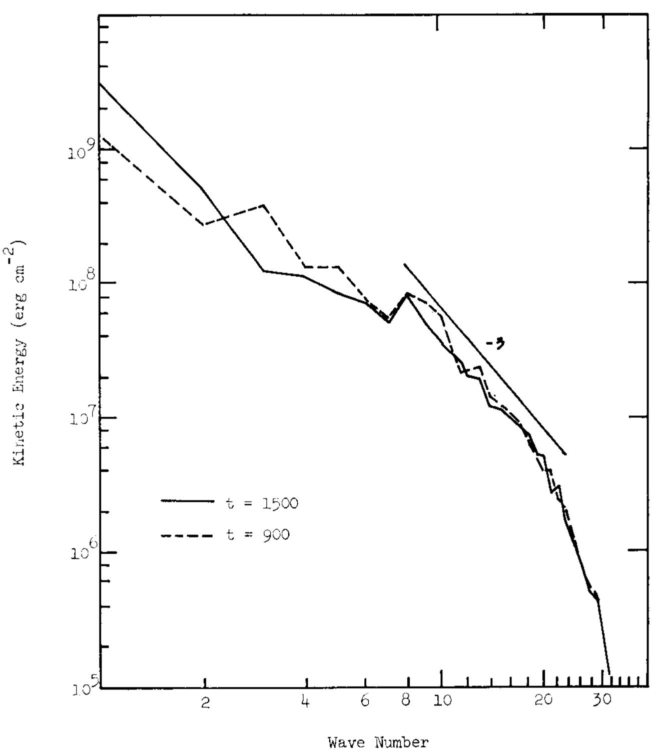

Fig. 8b. K_e spectra at $t = 900$, 1 500, Case B.

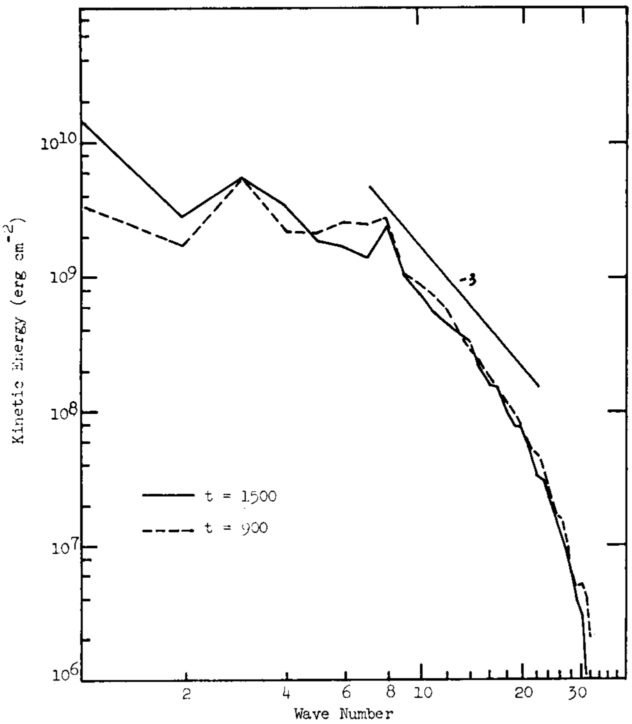

Fig. 8c. K_e spectra at $t = 900$, 1 500, Case C.

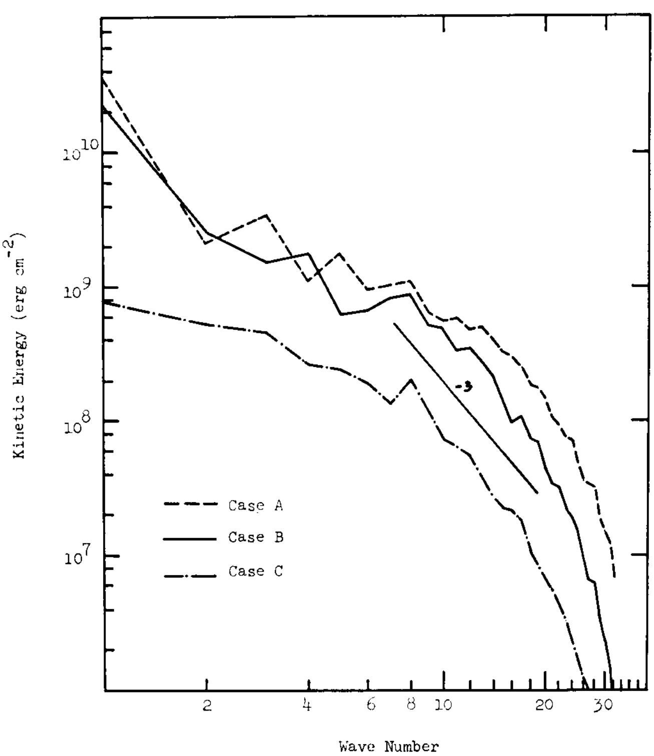

Fig. 9. K_e spectra at $t = 1$ 200 for Cases A, B, and C.

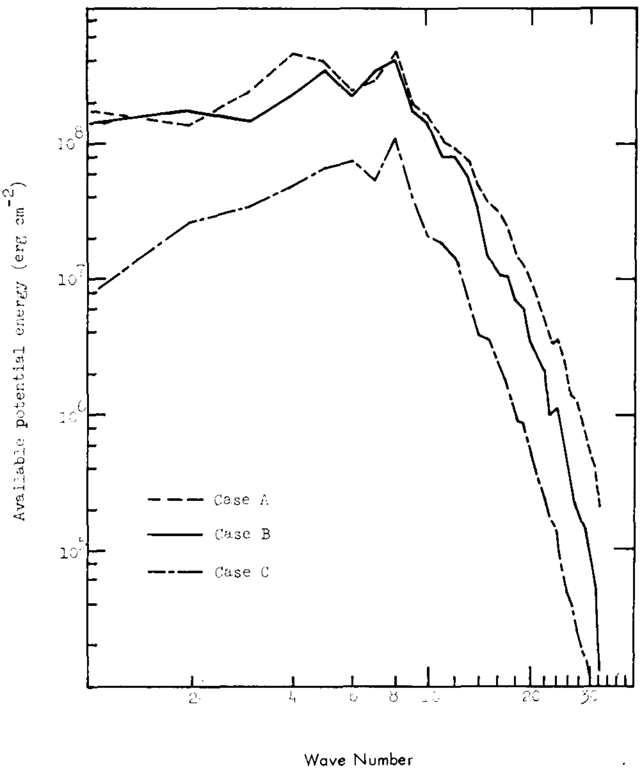

Fig. 10. The spectra of A_e at $t = 1\,200$ for Cases A, B, and C.

are all of the same order of magnitude for $8 \leqslant m \leqslant 16$. In Cases B and C which more closely resemble the atmosphere with respect to spectral slope of kinetic energy, the nonlinear transfer of K_e contributes the smallest effect to the kinetic energy budget. The relative effects of $C_K(m\,|\,n, l)$ and $C(A_e, K_e)$ correspond qualitatively to the results obtained from atmospheric data (Yang, 1967; Wiin-Nielsen, 1959).

In the three cases shown here, three somewhat different quasi-stationary spectral slopes are obtained. These vary from about -1.7 to -3.4 depending upon both the intensity of energy input and dissipation. In none of the cases is an "enstrophy inertial subrange" observed. It must be noted that results for $m > 16$ should be heavily qualified due to the possibility of aliasing, although the aliasing recognized in Lilly's (1969) experiments does not seem evident here. This may be due to the value of ν.

Looking at the available observational results without globally averaging, it would seem that the spectral slope of kinetic energy for $7 < m \leqslant 15$ varies between -2 and -4 depending on pressure, latitude and time. Perhaps the more fundamental underlying parameters are the intensity of energy production and dissipation. A brief glimpse of the possible effects of these two processes on the spectral slope has been presented. Three quasi-stationary spectral slope varying from -1.8 to -3.3 have been obtained. It may be of interest to probe the dependency of this slope on H and ν more fully.

Future gridpoint experiments should implement Orzag's (1971) suggestion of filtering out waves of $\lambda \leqslant 3\Delta x$, thereby producing, in the present case, an aliasfree spectrum of 21 components. Another feature which should be investigated is the effect of using a more complex and, most likely, more realistic formulation for dissipation. Possible choices are the formulation of Charney (loc. cit.) and Everson & Davies (1970). The difficulty involved may be indicated by the fact that the dissipation mechanism used by Smagorinsky (1965) based on inertial subrange argument, nevertheless results in relatively greater dissipation at small wavenumbers (Manabe et al., 1970).

By virtue of the dominance of the baroclinic process $C(A_e, K_e)$, for $8 \leqslant m \leqslant 16$, specifically, and Leith's (1968) suggestion that a -3 power law may be derived on dimensional grounds alone, avoiding the inertial subrange assumption it seems that C_i, the imaginary part of the phase speed commonly used in baroclinic instability studies may be used as a basis for explaining the spectral slope. Arguments for this case have recently been proposed (Steinberg, 1972).

Acknowledgements

I am indebted to Professor A. C. Wiin-Nielsen for his many suggestions throughout this work. My thanks to James Pfaendtner and Margaret Drake for valuable programming assistance.

This work was supported by The National Science Foundation Grant No. GA-16166. Computer time was supplied by the National Center of Atmospheric Research, which is sponsored by the National Science Foundation.

REFERENCES

Arakawa, A. 1966. Computational design for long-term numerical integration of the equations of fluid motion: two-dimensional incompressible flow, Part I. *J. Comp. Physics 1*, 119–143.

Baer, F. 1972. An alternate scale representation of atmospheric energy spectra. *J. Atmos. Sci. 29*, 649–664.

Batchelor, G. K. 1969. Computation of the energy spectrum in homogeneous two-dimensional turbulence. *Phys. Fluids Suppl.* II, *12*, II-233–II-239.

Charney, J. G. 1971. Geostrophic turbulence. *J. Atmos. Sci. 28*, 6, 1087–1095.

Charney, J. G. & Stern, M. E. 1961. On the stability of internal baroclinic jets in a rotating atmosphere. *J. Atmos. Sci. 19*, 159–172.

Derome, J. F. & Wiin-Nielsen, A. 1966. On the baroclinic stability of zonal flow in simple model atmospheres. The University of Michigan, Technical Report 06372-2-T.

Everson, P. J. & Davies, O. R. 1970. On the use of a simple two-level model in general circulation studies. *Quart. J. R. Met. Soc. 96*, 404–412.

Fjørtoft, R. 1953. On the changes in the spectral distribution of kinetic energy for the two-dimensional, nondivergent flow. *Tellus 5*, 225–230.

Horn, L. H. & Bryson, R. A. 1963. An analysis of the geostrophic kinetic energy spectrum of large-scale atmospheric turbulence. *J. Geophys. Res. 68*, 1059–1064.

Julian, P., Washington, W., Hembree, L. & Ridley, C. 1970. On the spectral distribution of large-scale atmospheric kinetic energy. *J. Atmos. Sci. 27*, 376–387.

Kao, S.-K. 1970. Wavenumber frequency spectra of temperature in the free atmosphere. *J. Atmos. Sci. 27*, 1000–1007.

Kraichnan, R. H. 1967. Inertial ranges in two-dimensional turbulence. *Phys. Fluids 10*, 1417–23.

Lawniczak, G. E., Jr. 1969. On a multiple-layer analysis of atmospheric diabatic processes and the generation of available potential energy. The University of Michigan, Technical Report 08759-5-T, 111 p.

Leith, C. E. 1968. Diffusion approximation for two-dimensional turbulence. *Phys. Fluids 11*, 671–673.

Lilly, D. K. 1965. On the computational stability of numerical solutions to the time dependent nonlinear geophysical fluid dynamics problems. *Mon. Wea. Rev. 93*, 11–26.

Lilly, D. K. 1969. Numerical simulation of two-dimensional turbulence. *Phys. Fluids Suppl.* II, *12*, II-240–II-249.

Manabe, S., Smagorinsky, J., Holloway, J. L. Jr & Stone, H. M. 1970. Simulated climatology of a general circulation model with a hydrological cycle. *Mon. Wea. Rev. 98*, No. 3, 175–212.

Merilees, P. E. & Warn, T. 1972. The resolution requirements of geostrophic turbulence. *J. Atmos. Sci. 29*, 990–991.

Orzag, S. A. 1969. Numerical methods for the simulation of turbulence. *Phys. Fluids Suppl.* II, *12*, II-250–II-257.

Orzag, S. A. 1971. On the elimination of aliasing in finite difference schemes by filtering high-wave-number components. *J. Atmos. Sci. 28*, 6, 1074.

Phillips, N. A. 1956. The general circulation of the atmosphere: a numerical experiment. *Quart. J. Roy. Meteor. Soc. 82*, 123–164.

Phillips, N. A. 1963. Geostrophic motion. *Rev. Geophys. 1*, 123–176.

Saltzman, B. 1970. Large scale atmospheric energetics in the wave number domain. *Rev. Geophys. Space Phys. 8*, 289–302.

Saltzman, B. & Fleischer, A. 1960. The modes of release of available potential energy in the atmosphere. *J. Geophys. Res. 65*, 1215–1222.

Saltzman, B. & Fleischer, A. 1961. Further statistics of the modes of release of available potential energy. *J. Geophys. Res. 66*, 2271–2273.

Saltzman, B. & Teweles, S. 1964. Further statistics on the exchange of kinetic energy between harmonic components of the atmospheric flow. *Tellus 16*, 432–435.

Smagorinsky, J. 1963. General circulation experiments with the primitive equations: 1. The basic experiment. *Mon. Wea. Rev. 91*, 991–1964.

Steinberg, H. L. 1971. On the power laws and nonlinear cascades in large scale atmospheric flow. The University of Michigan, Technical Report 002630-4-T.

Steinberg, H. L. 1972. On the power law for the kinetic energy spectrum of large scale atmospheric flow. *Tellus 24*, 288–292.

Steinberg, H. L., Wiin-Nielsen, A. & Yang, C. H.

1971. On nonlinear cascades in large-scale atmospheric flow. *J. Geophys. Res. 76*, 8629–8640.
Wellck, R. E., Kasahara, A., Washington, W. M. & De Santo, G. 1971. Effect of horizontal resolution in a finite-difference model of the general circulation. *Mon. Wea. Rev. 99*, 673–683.
Wiin-Nielsen, A. 1959. A study of energy conversion and meridional circulation for the large-scale motion in the atmopshere. *Mon. Wea. Rev. 87*, 319–332.
Wiin-Nielsen, A., Brown, J. A. & Drake, M. 1964. Further studies of energy exchange between the zonal flow and the eddies. *Tellus 16*, 168–180.
Wiin-Nielsen, A. 1967. On the annual variation and spectral distribution of atmospheric energy. *Tellus 19*, 540–559.
Yang, C. H. 1967. Nonlinear aspects of the large-scale motion in the atmosphere. The University of Michigan, Technical Report 08759-1-T.

ЧИСЛЕННОЕ МОДЕЛИРОВАНИЕ КВАЗИГЕОСТРОФИЧЕСКОЙ ТУРБУЛЕНТНОСТИ

Численно изучается эволюция турбулентности путем использования упрощенной двухуровенной квазигеострофической модели. Область, занимаемая жидкостью, содержит 64×64 точек сетки на одном уровне и удовлетворяет периодическим граничным условиям по x и по y. Турбулентность генерируется функцией нагревания, образованной двумерными Фурье-компонентами с большим волновым числом $m = 8$. Исследуются три случая для двух значений H-амплитуды функции нагревания и двух значений γ-коэффициента вихревой вязкости. В каждом случае получаются квазистационарные спектры. Наклоны спектров для $8 \leqslant m \leqslant 16$ в логарифмической шкале изменяются от $-1{,}7$ до $-3{,}4$ в зависимости от γ и H. Найдено, что нелинейный каскад доступной потенциальной энергии направлен в сторону больших волновых чисел. Нелинейный каскад кинетической энергии направлен от интервала $8 \leqslant m \leqslant 14$ к интервалу $1 \leqslant m \leqslant 7$, т. е. к большим масштабам. Приток энергии к компонентам с $m > 14$ в результате каскадного процесса относительно мал. Эти переносы находятся в качественном согласии с атмосферными наблюдениями. Притоки энстрофии довольно постоянны в интервале $14 \leqslant m \leqslant 28$. В инерционном интервале они должны быть нулями. Относительно малые притоки отмечены при $m < 7$, тогда как спектральный интервал $8 \leqslant m \leqslant 14$ действует как источник. За исключением волнового числа, разделяющего отрицательные и положительные значения, распределение оттоков и притоков энстрофии за счет инерционного каскада подобно тому, что получается из вычислений, основанных на атмосферных наблюдениях. Можно заключить, что теории двумерной турбулентности, сформулированные Фьюртофтом, Крейкнаном и Лейсом, имеют отношение к данной модели и атмосфере (в той мере, в какой наша модель напоминает атмосферу) в смысле предсказания главного направления нелинейного каскада кинетической энергии и энстрофии по спектру. Инерционный интервал, в котором каскад приводит к нулевым изменениям, не наблюдался ни в численных экспериментах данного исследования, ни в вычислениях, основанных на атмосферных наблюдениях в спектральном интервале $8 \leqslant m \leqslant 16$. Эксперименты, описанные в этой статье, были выполнены до появления теории Чарни и поэтому не могут рассматриваться как её проверка. Однако, некоторые допущения и выводы обсуждаются в свете этой теории.